Fine-Tuning of Patterns Assignment to Subnetworks Increases the Capacity of an Attractor Network Ensemble

Mario González[1(✉)], Ángel Sánchez[2], David Dominguez[3], and Francisco B. Rodríguez[3]

[1] SI2Lab, Universidad de las Américas, Quito, Ecuador
mario.gonzalez.rodriguez@udla.edu.ec
[2] E.T.S. Ingeniería Informática, Universidad Rey Juan Carlos, 28933 Madrid, Spain
angel.sanchez@urjc.es
[3] Grupo de Neurocomputacin Biolgica, Dpto. de Ingeniera Informtica, Escuela Politcnica Superior, Universidad Autónoma de Madrid, 28049 Madrid, Spain
{david.dominguez,f.rodriguez}@uam.es

Abstract. It is known that dividing an attractor network into a set of subnetworks whose connectivity is equivalent to the attractor network from which they come, and therefore with the same computational cost, increases the system's recovery capacity. This opens the possibility of optimizing the assignment of pattern subsets to the ensemble modules. The patterns subsets assignment to the network modules can be considered as a combinatorial optimization problem, where varied strategies (i.e. random vs. heuristic assignments) can be tested. In this work, we present a possible heuristic strategy driven by an overlap minimization in the subsets for assigning the patterns input to the modules of the ensemble attractor neural network. In terms of system pattern storage capacity, the assignment driven by the overlap minimization in each subset/module proved to be better than no specific assignment, i.e. distribution of patterns to modules randomly.

Keywords: Ensemble of diluted modules · Structured patterns · Retinal images retrieval · Module input optimization · Overlap driven assignment

1 Introduction

Attractor networks possess many desirable properties, they are dynamical systems able to store patterns (as fixed points) and retrieve information, starting from a stimulus similar to a pattern learned (inside the basin of attraction) [2,15]. Such properties are very useful in scenarios such as pattern denoising and pattern reconstruction. However, the storage capacity of the attractor model is limited, and even more, when patterns are correlated [14]. We have proposed an

I. Rojas et al. (Eds.): IWANN 2021, LNCS 12862, pp. 236–247, 2021.
https://doi.org/10.1007/978-3-030-85099-9_19

Ensemble Attractor Neural Network (EANN) [12] and proved that the retrieval capacity increases (almost triple) when compared with a single attractor network, while keeping the connectivity and computation cost the same [4,10–13]. We have tested the EANN for random unbiased patterns [11,12], as well for structured and biased patterns [4,10,13]. The ensemble attractor learner follows a divide-and-conquer approach, where the attractor network is divided into modules of diluted connectivity. The set of patterns, to feed the EANN, is divided into uniform subsets according to the number of modules in the ensemble, and each pattern subset is assigned to each module. The patterns supplied to each module are randomly chosen from the complete set of patterns to be stored in the EANN. In [13], we explored the ensemble model for fingerprint ridges patterns, finding an optimization of the retrieval capacity in terms of the ensemble components (modules) and connection topology. The retrieval capacity was non-monotonic in terms of the number of modules, and the optimum number of modules (ensuring maximum storage capacity) was found. Given that fingerprint ridges have a two-dimensional (2D) structure, a 2D cross grid topology performed better than a 1D ring topology. The small-world connectivity was also optimized for both 1D and 2D topologies for the attractor ensemble [13].

In this work, we present preliminary results of exploring the EANN in terms of optimizing the input strategy of pattern subsets to modules, following different strategies. The Digital Retinal Images for Vessel Extraction (DRIVE) Dataset [17] is used as input of the EANN system. The DRIVE contains spatially structured patterns, which implies a correlation between patterns. The EANN results helpful for dealing with such patterns. First, an optimization assignment problem arises, i.e. how the pattern subsets are assigned to the ensemble modules, where different assignment strategies can be tested. Second, a pre-processing, semi-supervised-like scenario, where the patterns subsets can be constructed so that each ensemble module, specializes and improves the retrieval for each assigned subset. The EANN has proved to increase the capacity of the single attractor. Given the divide-and-conquer approach of the ensemble learner when partitioning the set of patterns to be assigned to the ensemble modules, we prove that these subsets assignment can be used to improve the retrieval capacity by taking into account the non-homogeneous correlation among patterns within the subsets. This can be handled as an optimization combinatorial problem (i.e., an assignment problem), where a random assignment is compared to an heuristic strategy driven by overlap balancing. Intuitively, the goal of this strategy is to control the correlation equilibrium by minimizing the mean overlap among the patterns within subsets which are assigned to the different modules of the ensemble. In this way, all the modules in the EANN will have a load of patterns as balanced as possible in relation to the correlation (overlap) among the patterns to be stored. In this work, we show how this preprocessing strategy allows the subsets to be assigned by minimizing the correlation/similarity between patterns within each subset, and thus increasing the pattern storage capacity of the EANN.

2 Neural Model

This section presents the neural coding and network dynamics for each individual ensemble module, followed by a schematic representation of the ensemble model.

2.1 Neural Coding and Network Dynamics

The ensemble base learner (module) can be formalized as an attractor network, where the neural state is defined, at any discrete time t, by a set of N binary variables $\boldsymbol{\tau}^t = \{\tau_i^t \in 0,1; i = 1,\ldots,N\}$, where 1 and 0 represent, respectively, active and inactive states. The network will recover a set of patterns $\{\boldsymbol{\eta}^\mu,\ \mu = 1,\ldots,P\}$ that have been stored by a learning process. Each patter corresponds a stable fixed point attractor and the network retrieval state satisfies $\boldsymbol{\tau}^t = \boldsymbol{\eta}^\mu$, for large enough time t. The patterns in the DRIVE dataset are encoded as a set of binary variables $\boldsymbol{\eta}^\mu = \{\eta_i^\mu \in 0,1; i = 1,\ldots,N\}$, according to the probability $p(\eta_i^\mu = 1) = a,\ p(\eta_i^\mu = 0) = 1-a$. Where $a \in (0, 0.5]$ stands for the corresponding average activity ratio of the patterns [6,8].

The synaptic couplings between the neurons i and j are given by the adjacency matrix $J_{ij} \equiv C_{ij}W_{ij}$, where the topology matrix $\boldsymbol{C} = \{C_{ij}\}$ describes the connectivity structure of the neural network and $\boldsymbol{W} = \{W_{ij}\}$ is the matrix with the learning weights. The topology matrix corresponds to an asymmetric random network [1], with a network degree of K, that is each node is connected to a mean of K other nodes. The network is then characterized by the dilution parameter $\gamma = K/N$.

The retrieval of a gesture pattern is achieved through the noiseless neuron dynamics

$$\tau_i^{t+1} = \Theta(h_i^t - \theta_i^t)\,, \quad i = 1,\ldots,N\,, \tag{1}$$

where

$$h_i^t \equiv \frac{1}{K}\sum_j J_{ij}\frac{\tau_j^t - q_j^t}{\sqrt{Q_j^t}} \tag{2}$$

denotes the local field at neuron i and time t and θ_i is its threshold of firing. In Eq. (2) is introduced the average activity of the neighborhood of neuron i, $q_i^t = \langle\tau^t\rangle_i$, and its corresponding variance, $Q_i^t = Var(\tau^t)_i = \langle(\tau^t)^2\rangle_i - \langle\tau^t\rangle_i^2$. The neighborhood average is defined as $\langle f^t\rangle_i \equiv \sum_j C_{ij}f_j^t/K$. In Eq. (1) is used the step function $\Theta(x) = 1$ if $x \geq 0$, and $\Theta(x) = 0$, otherwise.

The uniform binary neural model is recovered when $a = 1/2$ [7].

In the sequel the normalized variables are used, the site and time dependence being implicit:

$$\sigma \equiv \frac{\tau - q}{\sqrt{Q}},\ q \equiv \langle\tau\rangle,\ Q \equiv Var(\tau) = q(1-q), \tag{3}$$

$$\xi \equiv \frac{\eta - a}{\sqrt{A}},\ a \equiv \langle\eta\rangle,\ A \equiv Var(\eta) = a(1-a), \tag{4}$$

where a and q are the pattern and neural activities, respectively. The averages done run over different groups of neurons, and are indicated in each case.

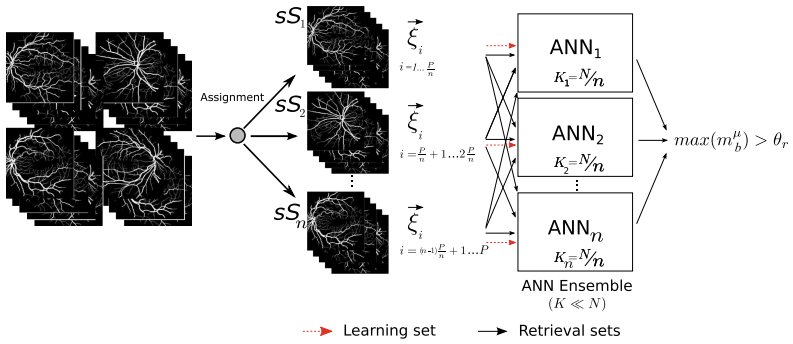

Fig. 1. Schematic representation of the assignment of patterns to the modules of the ensemble of diluted attractor neural networks.

In terms of these normalized variables, the neuron dynamics can be written as

$$\sigma_i^{t+1} = g(h_i^t - \theta_i^t, q_i^t); \quad h_i^t \equiv \frac{1}{K}\sum_j J_{ij}\sigma_j^t,\ i = 1, \ldots, N, \tag{5}$$

where the gain function is given by $g(x, y) \equiv [\Theta(x) - y]/\sqrt{y(1-y)}$.

The weight matrix $\boldsymbol{W}$ is updated according to the Hebb's rule, $W_{ij}^{\mu} = W_{ij}^{\mu-1} + \xi_i^{\mu}\xi_j^{\mu}$. Weights start at $W_{ij}^0 = 0$ and after P learning steps, they reach the value $W_{ij} = \sum_{\mu}^{P} \xi_i^{\mu}\xi_j^{\mu}$. The network learns $P = \alpha K$ patterns, where α is the load ratio. A threshold is necessary to keep the neural activity close to that of the learned patterns, $\theta^0(a) = \frac{1-2a}{2\sqrt{A}}$ is used, where a corresponds to the mean activity of the learning pattern set, and $A = a(1-a)$ to the activity variance. The threshold changes dynamically in time step t, according to the local neighborhood activity q_i^t, $\theta_i^t(q_i^t) = \theta^0(-\theta^0),\ q_i^t < 0.5 (> 0.5)$.

In order to characterize the retrieval ability of the network modules, the overlap is used, $m \equiv \frac{1}{N}\sum_i^N \xi_i\sigma_i$, which are the statistical correlation between the learned pattern ξ_i and the neural state σ_i.

2.2 Ensemble Attractor Network

Figure 1 depicts schematically the ensemble of attractor neural networks. The single attractor of size $N \times K$, where N is the number of units in the network and K the mean connectivity of each unit. One can see in Fig. 1 that network has been divided in an ensemble of n modules with connectivity K/n, and each module is assigned with a pattern subset. Note that the connectivity in each ANN module is highly diluted with $K \ll N$. It is well-known that diluted networks (K connections per unit instead of N connections, with $K \ll N$), increase the capacity of the attractor network per connection, and additionally the computation is less intensive (each local field only involves a K neighborhood activation) [3,5,12]. This works emphasizes in the assignment process, where the pattern dataset is also divided in n subsets, which will be assigned to each one of the n modules in the ensemble. To evaluate the ensemble performance, the

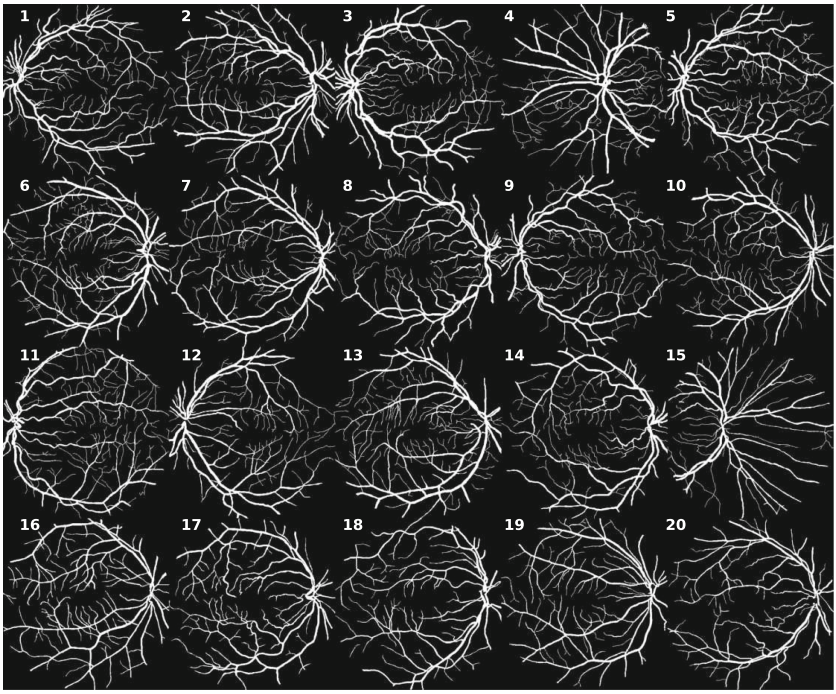

Fig. 2. Binarized and cropped Digital Retinal Images for Vessel Extraction (DRIVE) Dataset. The pattern (image) size is $530 \times 514 = 272420$, which is also the network size N.

retrieval efficiency R is defined as the number of learned patterns that are successfully retrieved $R = \frac{P_r}{P}$, where P_r is the overall number of retrieved patterns that satisfy $m^\mu > \theta_r$, and P is the overall number of patterns presented to the network during the learning phase. One has that $P \geq P_r$. Here, $\theta_r = 0.7$ is used as the retrieval threshold, unless stated otherwise. The mean retrieval overlap M is calculated over all patterns subset $\mu \in 1, 2, \ldots, P$, $M = \langle m \rangle_\mu = 1/P \sum_{\mu=1}^{P} m^\mu$. It is worth noting that in the case of the ensemble, the retrieval pattern load is calculated as $\alpha_R = \frac{P_r}{K_b \times n}$ where n is the number of subnetworks. Thus, we use $K_b \times n = K$ constant for all network ensembles studied, where K is the connectivity of the single "dense" network.

3 Materials and Methods: Approach for the Considered Assignment Problem

3.1 Dataset: Characterization and Analysis of Overlap

Figure 2 depicts the processed dataset used to test the ensemble learning. The patterns come from the Digital Retinal Images for Vessel Extraction (DRIVE) Dataset [17]. This dataset is commonly used for segmentation of blood vessels in retinal images. Retina vascular patterns is a well-known a biometric trait for

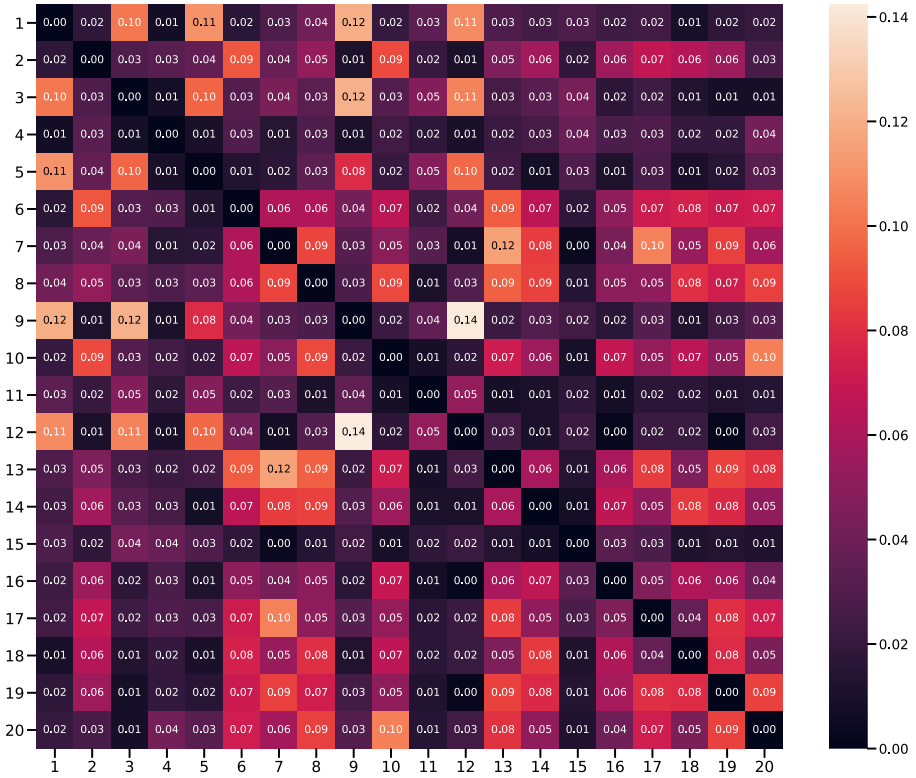

Fig. 3. Overlap matrix $O^{\mu\nu}$ between all patterns in the binarized DRIVE dataset, t, calculated through Eq. 6.

accurate authentication of people but it is also one of the least deployed due to a very low acceptability [18]. The dataset contains 40 images of which 20 have been manually segmented. These 20 images have also been binarized and the image edges with no information have been removed (cropped). The resulting binary patterns are shown in Fig. 2. Each digital retinal image has a size of $530 \times 514 = 272420$ pixels and the size of the pattern is the same as the number of neurons that each ensemble module contains. Thus, the dataset is comprised of $P = 20$ patterns (binary images), of size $N = 272420$.

Figure 3 represents the overlap matrix corresponding to the DRIVE dataset. The overlap matrix entries can be defined as:

$$O^{\mu\nu} = \frac{1}{N} \sum_{i}^{N} \xi_i^{\mu} \cdot \xi_i^{\nu}. \tag{6}$$

The resulting overlap matrix is of size $P \times P$, with $P = 20$. The overlap of a pattern μ with itself, that is the entries of the overlap matrix, where, $\mathbf{O}^{\mu\nu} = 1$, $\forall \mu = \nu$. For the purpose of calculating the overlap of each pattern with the rest of the dataset, the overlap of a pattern with itself must be removed. One can

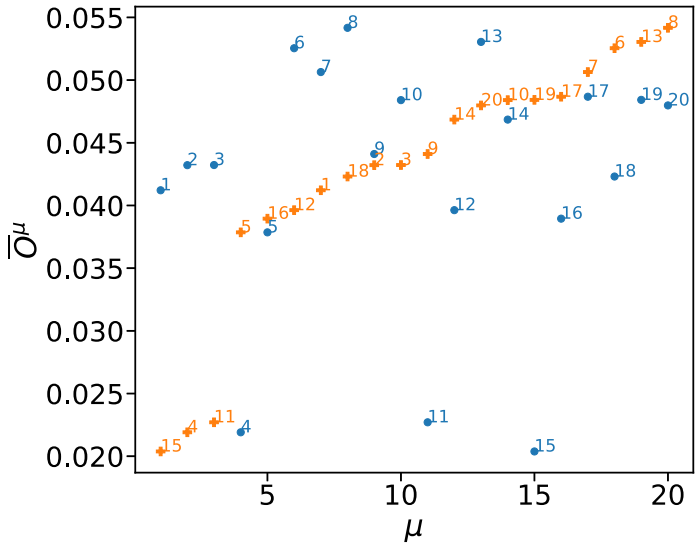

Fig. 4. Mean Overlap of each pattern μ with the rest of $P-1$ patterns, $\overline{O}^{\mu}$, for the DRIVE dataset. The orange crosses represent the patterns ordered from least mean overlap to greatest mean overlap between one pattern and the rest. The blue dots represent a random realization of the mean overlaps for the 20 retinal images patterns.

observe, that the overlap between patterns in the dataset reaches values of at most $\mathbf{O}^{\mu=9,\nu=12} = 0.14$, for patterns $\mu = 9,\ \nu = 12$. This is a non-negligible value for the cross-talk noise term, which worsens the performance of the attractor network.

Figure 4 shows the mean overlap of pattern μ with the $P-1$ patterns in the DRIVE dataset, which can be defined as:

$$\overline{O}^{\mu} = \frac{1}{P}\sum_{\nu=1}^{P} O^{\mu\nu},\ \nu \neq \mu. \tag{7}$$

That is the sum of each row of the overlap matrix in Fig. 3 over the $P-1$ patterns. The mean overlap of each pattern with the rest of the dataset, $\overline{O}^{\mu}$ can be used as a criterion to assign the patterns to the modules in the ensemble. In Fig. 4, the patterns are depicted according their mean overlap with the dataset. In blue dots, the patterns are presented following a random order. In orange crosses, the patterns are presented from minimum to maximum mean overlap with the rest of the patterns in the dataset. One can observe in this figure that patterns 15, 4, and 11 are the ones with lower mean correlation with respect to the rest of the dataset. Thus, a discontinuity in the mean overlap $\overline{O}^{\mu}$ occurs for the rest of the dataset, and this value then increases following an approximate linear behavior.

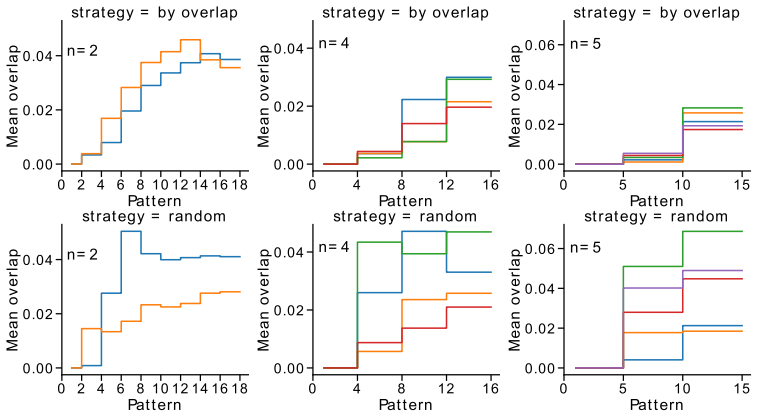

Fig. 5. Example of dynamic pattern assignment to network modules. The first row of panels ($n = 2,\ 4,\ 5$ modules), depicts the different selected sets reach a balanced state with similar average overlaps in each selected set. On the contrary, in the second row of panels ($n = 2,\ 4,\ 5$ modules), with the random strategy, the state of the final sets is clearly more unbalanced with respect to the average of each set of selected patterns.

3.2 Strategy for Assigning Patterns to Modules

Patterns subset assignment to network modules is a type of combinatorial assignment problem [16]. Our considered problem resembles the subset assignment problem which is applied to data placement in caches [9]. Given the organization of the attractor network into a fixed number of modules, and the partition of the patterns into disjoint subsets, an optimized subset-to-module assignment strategy is needed. This work describes a new pattern assignment strategy for the considered problem. The idea behind our strategy is based on the overlap value within each patterns subset. The patterns are assigned to a subset so that the overlap within each subset is as low and balanced as possible. The assignment algorithm is detailed as follows:

1 Calculate the overlap matrix **O**.
  Start **Pset** with all $P = 20$ binarized DRIVE patterns.
  Start each subset $(S_1, S_2, \ldots S_n)$ with a random seed and remove the seed from the original pattern set **Pset**.
2 Alternately assign a pattern to each subset S_i as follows:
  2.1 Select a pattern candidate μ^c from the remaining patterns in **Pset** and include it in subset S_i.
  2.2 Measure the overlap matrix of the subset (this is equivalent to get a section of the matrix $\mathbf{O}[S_i, S_i]$).
  2.3 Repeat 2.1 and 2.2 for all patterns' candidates μ^c, remaining in the **Pset**.
  2.4 Select as final candidate the pattern μ^c that produces the minimum overlap matrix for the subset, add it to S_i, and remove it from **Pset**.
3 Repeat 2 until no candidates in **Pset** are left.

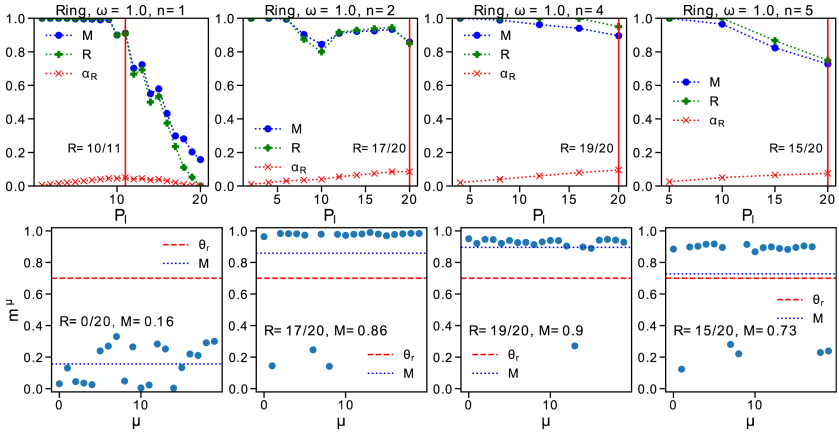

Fig. 6. Macroscopic and microscopic performance of the recovery of the set of 20 retinal images patterns for different number of modules in the EANN ($n = 1,\ 2,\ 4,\ 5$). Top row shows the EANN performance curves $M,\ R,\ \alpha_R$, the maximum value cut-off for the pattern load P, is indicated with the solid red vertical line, and the fraction of retrieved patterns $R = Pr/P$. Bottom row shows the microscopic retrieval of $P = 20$ retinal images patterns, that is the whole dataset is loaded in the network. This corresponds to the load in the last point of the top panels curves. This microscopic retrieval is shown for different number of modules ($n = 1,\ 2,\ 4,\ 5$). (Color figure online)

Note that this algorithm generates disjoint subsets of patterns in the assigning process to the modules of EANN.

The aforementioned process is represented in Fig. 5 for the DRIVE dataset for different number of modules, i.e. $n = \{2,\ 4,\ 5\}$. An initial pattern set $Pset$ with 20 binary images must be assigned to the n ensemble modules. Note that n has been chosen to be an exact divisor of **card**($Pset$). The assignment strategy driven by overlap (Fig. 5 top panels) is compared with a random assignment (Fig. 5 bottom panels). The assignment strategy driven by overlap allows a more balanced pattern subsets placing into modules, with the subsets having a similar mean overlap, as well as having a smaller mean overlap when compared with the random assignment. For the case of $n = 2$ modules (Fig. 5 left panels), the overlap is similar for both assignment strategies, however the assignment driven by overlap is more balanced. The effect is more noticeable for a larger number of subsets, as it can be observed in top middle and right panels of Fig. 5, where the value of the mean of the assignment driven by overlap is more distinguishable low than the random assignment for $n = 4$ and $n = 5$ modules.

4 Results

The tested attractor ensemble has $N = 272420$ nodes with total connectivity of $K = 200$, that is a dilution of $\gamma = K/N \approx 0.0007$, and the network topology connectivity is random. Figure 6 shows the retrieval performance

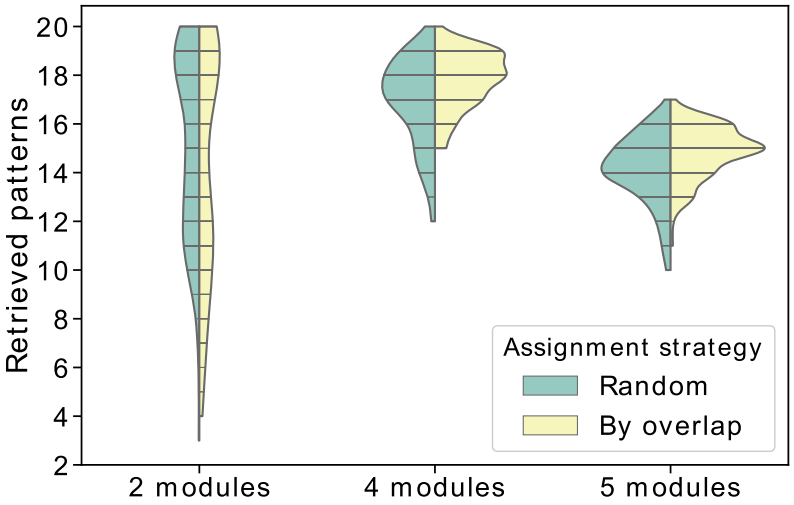

Fig. 7. Retrieval performance for different number of modules $n = 2,\ 4,\ 5$, and the two tested assignment strategies (random vs driven by overlap). A hundred realizations of the assignment process were carried out for each configuration and the retrieved number of patterns is compared.

for $n = 1,\ 2,\ 4,\ 5$ ensemble modules, corresponding to modules connectivity $K_b = K/n$ of $K_b = 200,\ 100,\ 50,\ 40$, respectively. Note that all systems are equivalent in terms of network size $N \times K_b \times n = 272420 \times 200$. For a single attractor module ($n = 1$) the optimal retrieval (red vertical line) occurs for a load of $P_l = 11$ patterns, being able to retrieve just $P_r = 10$ of them, as depicted in Fig. 6 top left panel. Loading the whole $P_l = 20$ patterns in a single module, none of them are retrieved (see Fig. 6 bottom-left panel), achieving a mean retrieval overlap of $M = 0.16$. This highlights the difficulties of learning correlated patterns as is the case with the DRIVE dataset.

Increasing the number of modules ($n = 2,\ 4,\ 5$) in the ensemble improves the retrieval capacity of the system. In [13], an optimal value appears for the number of modules n in the ensemble, for retrieving fingerprint patterns. In the case of the binarized DRIVE dataset, a maximum retrieval is achieved for $n = 4$ modules. A retrieval of $R = P_r/P_l = 19/20$ (quantity) patterns occurs with a mean retrieval overlap (quality) of $M = 0.9$. This value is higher than the observed for $n = 2$ modules, $R = 17/20$, $M = 0.86$, and for $n = 5$ modules, $R = 15/20$ $M = 0.73$. These preliminary results guarantee a more detailed analysis as the one carried out in [13].

Figure 7 compares both assignment strategies: random vs. driven by overlap. It summarizes the results of 100 simulations for the different cases studied, i.e. assignment strategies and number of modules. A violin plot is constructed comparing for each number of modules ($n = 2,\ 4,\ 5$) and the two assignment strategies (random and driven by overlap). The best results correspond to $n = 4$

modules, where the density plots tend to the maximum of the patterns in the dataset $P = 20$. The density curve peak moves towards the total number of patterns in the dataset $P = 20$ and becomes narrow near this value. This clearly shows a better retrieval capacity for $n = 4$ modules. A maximum value can be found ($n = 4$), and increasing further the number of modules worsen the retrieval performance. In practice, the connectivity dilution have a limit, where the modules connectivity worsen their performance [13]. Comparing for each module the two assignment strategies, random vs. driven by overlap, the latter performs better for the DRIVE dataset. Thus, an optimizing strategy for assigning the patterns to the modules, balancing the overlap between patterns in the subsets, improves the network performance. Again, this results need to be checked more extensively in a future work.

5 Conclusions

The attractor network ensemble has proved to increase the retrieval capacity when compared with a single attractor of similar connectivity. This has been observed for random and structured patterns. Structured patterns, such as retinal image vessels, are usually correlated. The correlation among patterns tampers the retrieval performance of the attractor network. The ensemble division into modules, which are assigned with disjoint pattern subsets help solving the correlation issue. In this work, an assignment strategy driven by the minimization of the overlap (correlation) between patterns belonging to each subset was tested. Since the problem of assigning pattern subsets to ensemble modules is a combinatorial problem, we intend to test diverse heuristic strategies and compare the performance of the network for different structured datasets. The strategy driven by overlap minimization was compared with a random assignment strategy, and proved to be better in terms of retrieval performance, achieving a larger number of retrieved patterns. The assignment problem considered in the present scenario for the attractor ensemble, can benefit of preprocessing the subsets, so that the pattern retrieval is maximized. An interesting issue is that there are a number of EANN modules where this strategy works best, which should be investigated in more detail in future work, depending on the specific topology of the subnetworks in the modules. On the other hand, a more extensive investigation of possible new strategies for assigning patterns according to other criteria is also needed for future work.

Acknowledgments. Funded by UDLA-SIS.MGR.21.04, AEI/FEDER TIN2017-84452-R, PID2020-114867RB-I00, RTI2018-098019-B-I00, and CYTED Network 518RT0559.

References

1. Albert, R., Barabási, A.L.: Statistical mechanics of complex networks. Rev. Mod. Phys. **74**(1), 47 (2002)

2. Amit, D.J.: Modeling Brain Function: The World of Attractor Neural Networks. Cambridge University Press, New York (1992)
3. Arenzon, J., Lemke, N.: Simulating highly diluted neural networks. J. Phys. A Math. Gen. **27**(15), 5161 (1994)
4. Dávila, C., González, M., Pérez-Medina, J.-L., Dominguez, D., Sánchez, Á., Rodriguez, F.B.: Ensemble of attractor networks for 2D gesture retrieval. In: Rojas, I., Joya, G., Catala, A. (eds.) IWANN 2019. LNCS, vol. 11507, pp. 488–499. Springer, Cham (2019). https://doi.org/10.1007/978-3-030-20518-8_41
5. Derrida, B., Gardner, E., Zippelius, A.: An exactly solvable asymmetric neural network model. EPL (Europhys. Lett.) **4**(2), 167 (1987)
6. Dominguez, D., González, M., Rodríguez, F.B., Serrano, E., Erichsen Jr., R., Theumann, W.: Structured information in sparse-code metric neural networks. Phys. A Stat. Mech. Appl. **391**(3), 799–808 (2012)
7. Dominguez, D., González, M., Serrano, E., Rodríguez, F.B.: Structured information in small-world neural networks. Phys. Rev. E **79**(2), 021909 (2009)
8. Doria, F., Erichsen Jr., R., González, M., Rodríguez, F.B., Sánchez, Á., Dominguez, D.: Structured patterns retrieval using a metric attractor network: application to fingerprint recognition. Phys. A Stat. Mech. Appl. **457**, 424–436 (2016)
9. Ghandeharizadeh, S., Irani, S., Lam, J.: The subset assignment problem for data placement in caches. Algorithmica **80**(7), 2201–2220 (2018)
10. González, M., Dávila, C., Dominguez, D., Sánchez, Á., Rodriguez, F.B.: Fingerprint retrieval using a specialized ensemble of attractor networks. In: Rojas, I., Joya, G., Catala, A. (eds.) IWANN 2019. LNCS, vol. 11507, pp. 709–719. Springer, Cham (2019). https://doi.org/10.1007/978-3-030-20518-8_59
11. González, M., Dominguez, D., Sánchez, Á., Rodríguez, F.B.: Capacity and retrieval of a modular set of diluted attractor networks with respect to the global number of neurons. In: Rojas, I., Joya, G., Catala, A. (eds.) IWANN 2017. LNCS, vol. 10305, pp. 497–506. Springer, Cham (2017). https://doi.org/10.1007/978-3-319-59153-7_43
12. Gonzalez, M., Dominguez, D., Sanchez, A., Rodriguez, F.B.: Increase attractor capacity using an ensembled neural network. Expert Syst. Appl. **71**, 206–215 (2017). https://doi.org/10.1016/j.eswa.2016.11.035
13. González, M., Sánchez, Á., Dominguez, D., Rodríguez, F.B.: Ensemble of diluted attractor networks with optimized topology for fingerprint retrieval. Neurocomputing **442**, 269–280 (2021)
14. Hertz, J.A., Krogh, J., Palmer, R.: Introduction to the Theory of Neural Computation. Santa Fe Institute Studies in the Sciences of Complexity, vol. 1. Addison-Wesley (1991)
15. Hopfield, J.J.: Neural networks and physical systems with emergent collective computational abilities. Proc. Nat. Acad. Sci. **79**(8), 2554–2558 (1982)
16. Pentico, D.W.: Assignment problems: a golden anniversary survey. Eur. J. Oper. Res. **176**(2), 774–793 (2007)
17. Staal, J., Abramoff, M., Niemeijer, M., Viergever, M., van Ginneken, B.: Ridge based vessel segmentation in color images of the retina. IEEE Trans. Med. Imaging **23**(4), 501–509 (2004)
18. Uhl, A.: State of the art in vascular biometrics. In: Uhl, A., Busch, C., Marcel, S., Veldhuis, R. (eds.) Handbook of Vascular Biometrics. ACVPR, pp. 3–61. Springer, Cham (2020). https://doi.org/10.1007/978-3-030-27731-4_1